Measurement of activation of helium gas by ^{238}U beam irradiation at about 11 A MeV

A. Akashio[a], K. Tanaka, H. Imao, and Y. Uwamino

RIKEN Nishina Center 2-1 Hirosawa, Wako, Saitama, Japan

Abstract. A new helium-gas stripper system has been applied at the ~11 A MeV uranium beam of the Radioactive Isotope Beam Factory of the RIKEN accelerator facility. Although the gas stripper is important for the heavy-ion accelerator facility, the residual radiation that is generated is a serious problem for maintenance work. The residual dose was evaluated by using three-layered activation samples of aluminium and bismuth. The γ-rays from produced radionuclides with in-flight fission of the ^{238}U beam and from the material of the chamber activated by neutrons were observed by using a Ge detector and compared with the values calculated by using the Monte-Carlo simulation code PHITS.

1 Introduction

The Radioactive Isotope Beam Factory (RIBF) of the RIKEN accelerator facility is used to generate intense beams of radioactive isotopes for use in studies on nuclear physics and nuclear astrophysics. The superconducting-ring cyclotron produces beams of heavy ions of nuclei ranging from hydrogen to uranium. The energy of the primary beam is about 350 MeV per nucleon, and the targeted intensity is as high as one particle microampere, corresponding to 6.2×10^{12} particles/s [1].

To accelerate a beam of uranium ions for use in generating a variety of radioactive nuclei, it is necessary to strip electric charges from the uranium ions by passing them through materials at an intermediate energy of 10–20 A MeV. Serious radiation damage caused by the high-intensity uranium beam causes problems with the lifetimes of solid materials; consequently, it is difficult to use solids in the electron stripper. This is common problem at high-intensity heavy-ion accelerator facilities.

At the RIBF, a helium-gas stripper system that changes the charge on the uranium ions from U^{35+} to U^{71+} has been successfully developed [2]. Because the stripper setup has to be changed for each ion nuclide, such as uranium, xenon, etc., the residual dose is a serious problem with respect to maintenance work. The intensity of the uranium beam at the target in operation in 2015 was 50 particle nanoamperes, and this will become more intense in the future. It is important to understand the origin of the high residual dose and to make plans to reduce the radiation dose during maintenance work.

Because gas stripper systems might become popular solutions for use in high-intensity accelerator facilities, the activation around the gas stripper chamber was measured by using activation samples. The activation of the stripper system, intended to provide a low activation of the setup, good shielding, and an effective maintenance process for future design, was evaluated by using the Monte-Carlo simulation code PHITS [3] and the results were compared with those obtained experimentally.

2 Experiment

Figure 1 shows the place of the helium gas stripper at RIBF, and Figure 2 is a schematic view of the helium-gas stripper setup used in the PHITS calculation. The energy of the uranium beam in the helium gas region was 10.75 MeV per nucleon, and the beam intensity was 0.86 particle microamperes. The helium-gas pressure in the region of highest pressure was 7 kPa, and the thickness of the helium layer was about 500 mm, which corresponds to 0.7 mg/cm^2. The beam intensity was measured nondestructively by a using phase probe [4]. The helium gas was irradiated with 5.4×10^{18} uranium ions (±20% accuracy) during about 18 days of operation of the accelerator.

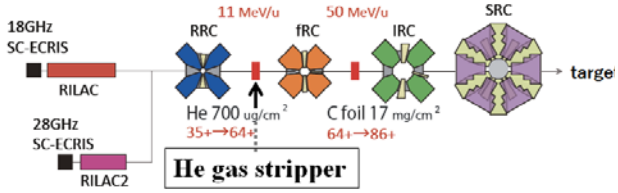

Figure 1. Place of the helium gas stripper setup at RIBF.

[a] Corresponding author: horigome@riken.jp

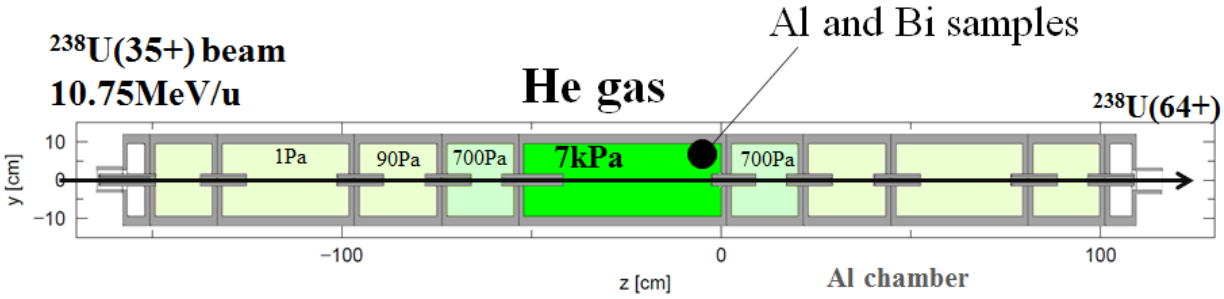

Figure 2. Schematic side-cross sectional view of the helium-gas stripper setup. The helium gas is contained in the gas cells. The uranium beam penetrates the centre of the chamber. Each cells are connected each other at the beam pass without any window. The highest pressure of the helium was 7k Pa.

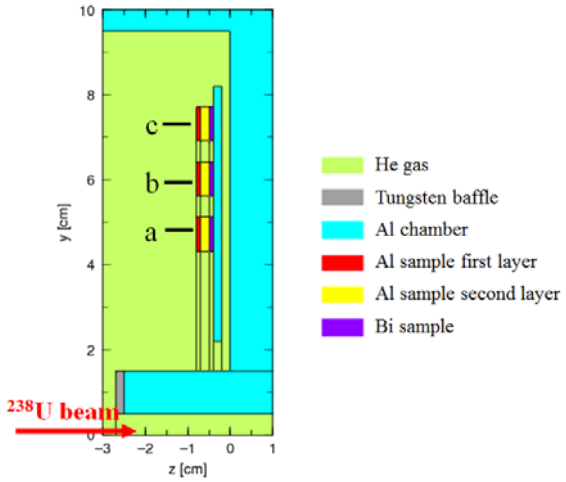

Figure 3. Expanded schematic view of Figure 2 around the sample position. Each samples consisted of three layers of the same three materials. The symbols a–c are assigned with respect to the beam line. The positions are indicated as Al-1a, Al-2a, and Bi-a for positions in the first, second, and third layers, respectively.

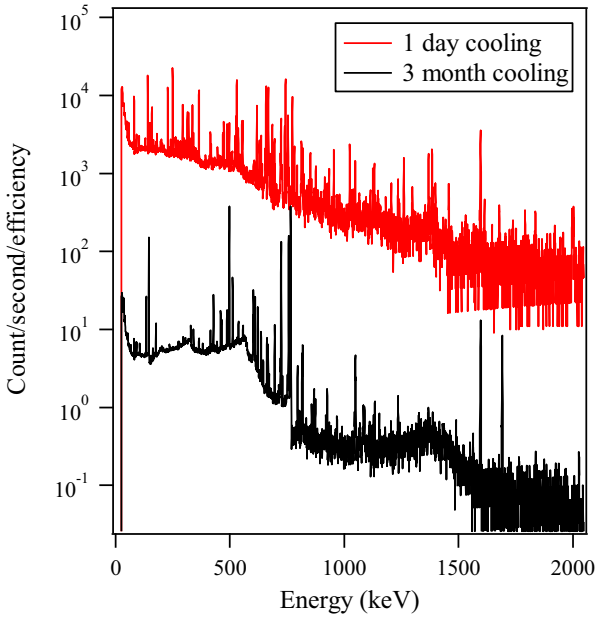

Figure 4. Typical γ-ray spectra of an Al sample set in the gas stripper chamber. The spectra were normalized with respect to the measurement time and the efficiency of the Ge detector. The red spectrum was recorded following 1 day of cooling after beam irradiation ceased, and the black spectrum was recorded after 3 months of cooling. Many of the energy peaks for short-lived radioactive isotopes generated by fission of ^{238}U showed a decrease after 3 months.

The activation samples were located inside the gas stripper chamber. Each sample consisted of three layers, the structure of which is shown in Figure 3. The first layer, consisting of a 1-mm-thick, 10 × 10 mm specimen of aluminium, was intended to catch the products of in-flight fission of the uranium beam. The second layer consisting of a 2-mm-thick, 10 × 10 mm specimen of aluminium was activated by neutrons only, because most of the fission products from the uranium beam were captured by the first layer. These aluminium specimens were used to evaluate the activation of the aluminium chamber of the gas stripper. The third layer of the sample consisted of 1-mm-thick, 10 × 10 mm specimen of bismuth. Bismuth isotopes generated from natural ^{209}Bi are sensitive to neutron energy, because of the low neutron-energy thresholds of their reactions. The uranium beam passed though the helium gas. The sample closest to the source of the beam inside the chamber was at a distance of 47.25 mm.

Figure 4 shows typical γ-ray spectra from the Al-1a sample, measured following about 1 day and 3 months of cooling time.

Because evaluation of radiation from long-lived isotopes is more important than that for short-lived isotopes, we performed our measurements after three months, so that the background level was reduced. The radioactive nuclei generated in the samples were identified and counted from the spectra, taking into account the efficiency and half-life. Table 1 lists the radioactive nuclei identified by γ-ray spectroscopy after the three-month cooling period, and mass distribution of the identified nuclei are shown in Figure 5. Typical fission-product nuclei from the uranium beam were observed. The long-lived isotope ^{22}Na was also observed; this was generated from the aluminium sample by neutron-induced reaction. Table 2 lists the observed bismuth isotopes, with their neutron-energy thresholds. 22.55 MeV neutrons were detected, whereas 28.64 MeV neutrons, which can generate ^{205}Bi

from ^{209}Bi, were not detected.

Table 1. Typical radioactive nuclei observed in the aluminium sample Al-1a from the stripper chamber after cooling for about 3 months.

Nuclide	Half-life	Nuclide	Half-life
^{91}Y	58.5 day	^{134}Cs	2.06 year
^{95}Zr	64.0 day	^{137}Cs	30.1 year
^{103}Ru	39.3 day	^{141}Ce	32.5 day
^{106}Ru	371 day	^{144}Ce	285 day
^{124}Sb	60.2 day	^{155}Eu	4.75 year
^{125}Sb	2.76 year		

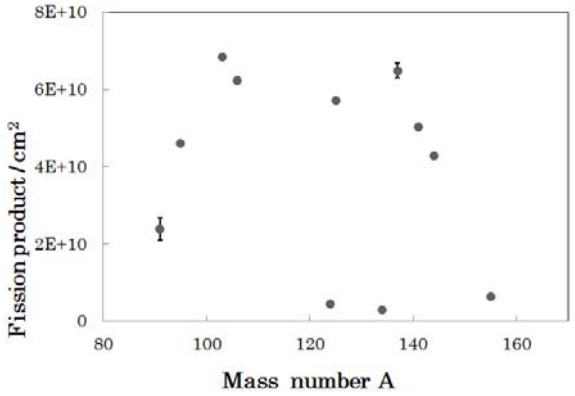

Figure 5. Mass distribution of the fission products observed in the aluminium sample Al-1a after the cooling for about 3 months. The low production of A = 124 and 134 were produced directly. The others are the summation of produced nuclei of the same mass because of the beta-decay, respectively as explained in Figure 8.

Table 2. Threshold of the neutron energy corresponding to the production of radioactive bismuth isotopes. ^{206}Bi, ^{207}Bi, and ^{208}Bi were observed in this study.

Nuclide	Half-life	Reaction	Threshold (MeV)
^{208}Bi	1.4×10^5 year	^{209}Bi(n,2n)^{208}Bi	
^{207}Bi	31.6 year	^{209}Bi(n,3n)^{207}Bi	14.12
^{206}Bi	6.4 days	^{209}Bi(n,4n)^{206}Bi	22.55
^{205}Bi	15.31 day	^{209}Bi(n,5n)^{205}Bi	29.62

3 PHITS calculation

The calculation was performed by using PHITS ver. 2.76 for the geometry shown in Figure 2. PHITS uses the JAERI Quantum Molecular Dynamics model for the nucleus–nucleus reaction of ^{238}U with helium. The Generalized Evaporation Model was used to simulate the evaporation and fission processes of the excited states, the INCL model was used for nucleon–nucleus collisions at energies above 20 MeV [3], and the JENDL-4 library of evaluated nuclear data was used to calculate collisions below 20 MeV [5].

Figure 6 shows the results of calculations of the fluxes of generated nuclei and neutrons. The fission products reached the position of the aluminium sample.

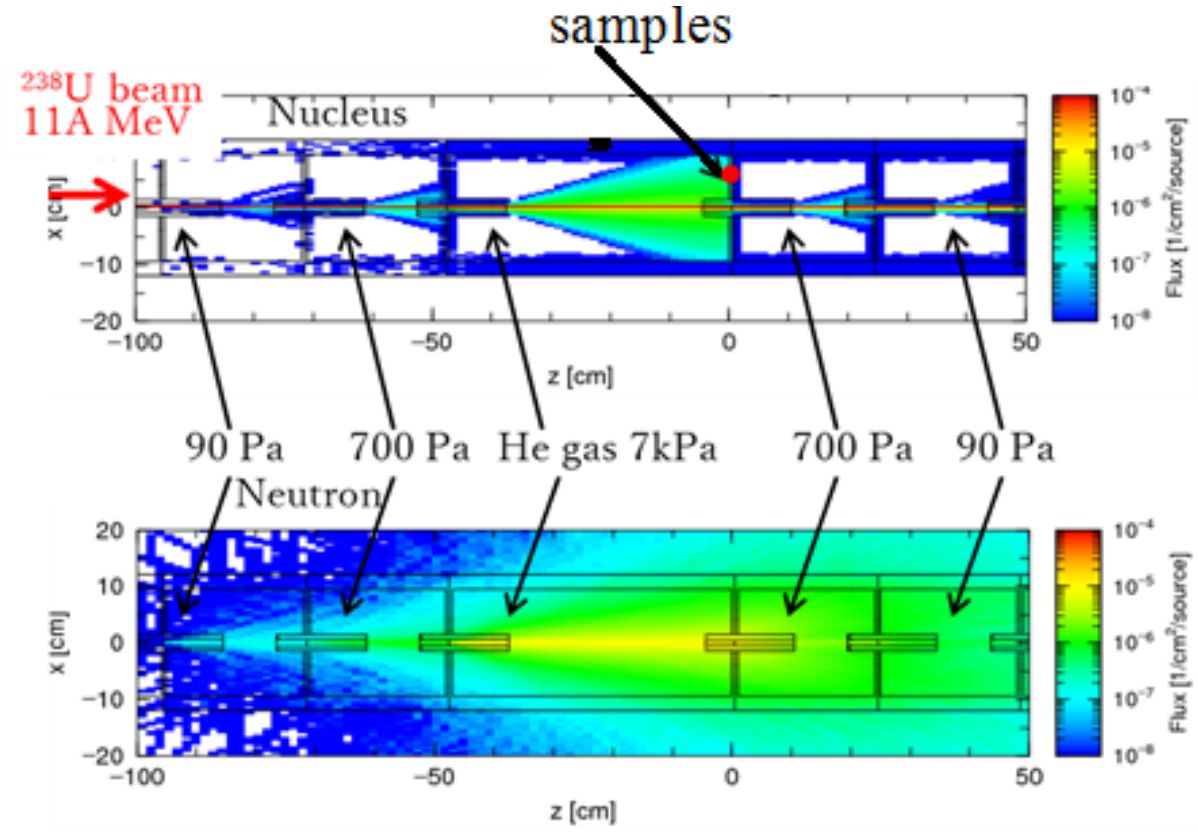

Figure 6. Cross-sectional view from above of the flux of generated nuclei (upper) and neutrons (lower), as calculated by PHITS

The sample sizes were small and it was difficult to obtain enough statistics of fission products and neutrons by PHITS calculation. To obtain enough statistics for the samples, ring-type samples were set in the PHITS geometry by the area as explained by D. Satoh et al [6]. Figure 7 shows the neutron spectrum irradiated to the aluminium sample Al-1a. The peak energy is the same as the uranium beam energy. About 90 % of the neutron were less than 20 MeV thus aluminium and bismuth activation by neutron was calculated by using the nuclear data, mainly.

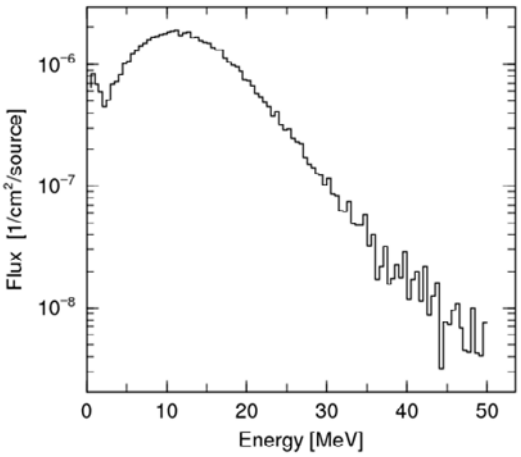

Figure 7. Neutron spectrum impinged to the sample Al-1a.

The numbers of nuclei that were stopped by the samples were counted, and the results were compared with the measured value. Although short-lived nuclei were also observed, we chose to examine long-lived nuclei in the evaluation of the activation because of their contribution to the residual dose in the experimental setup.

Figure 8 shows a nuclear chart of the PHTIS calculation results for radioactive nuclei produced in sample Al-1a for irradiation by 8×10^9 uranium ions. Short-lived nuclei were eliminated from the spectra measured after three months of cooling. Therefore, the numbers of short-lived nuclei deduced by PHITS were counted and summed to give the long-lived daughter nuclei shown in Figure 8.

Because the helium gas was about 50-cm thick, it was difficult to determine the angle of fission products against the samples, experimentally. From the calculation result, the average angles of the fission products to the first-layer specimens were 6°, 8°, and 10° for Al-1a, Al-1b, and Al-1c, respectively. Therefore, the angular property was evaluated with thin target case by PHITS calculation. Figure 9 shows angular distributions of neutron, cesium isotopes, and ruthenium isotopes which are typical fission products. The helium target was assumed as 1-mm thick and 0.7 mg/cm^2 as same as the stripper in this study. Because the angular difference of the samples estimated by PHITS calculation were small, angular dependence of the fission products yield were also small.

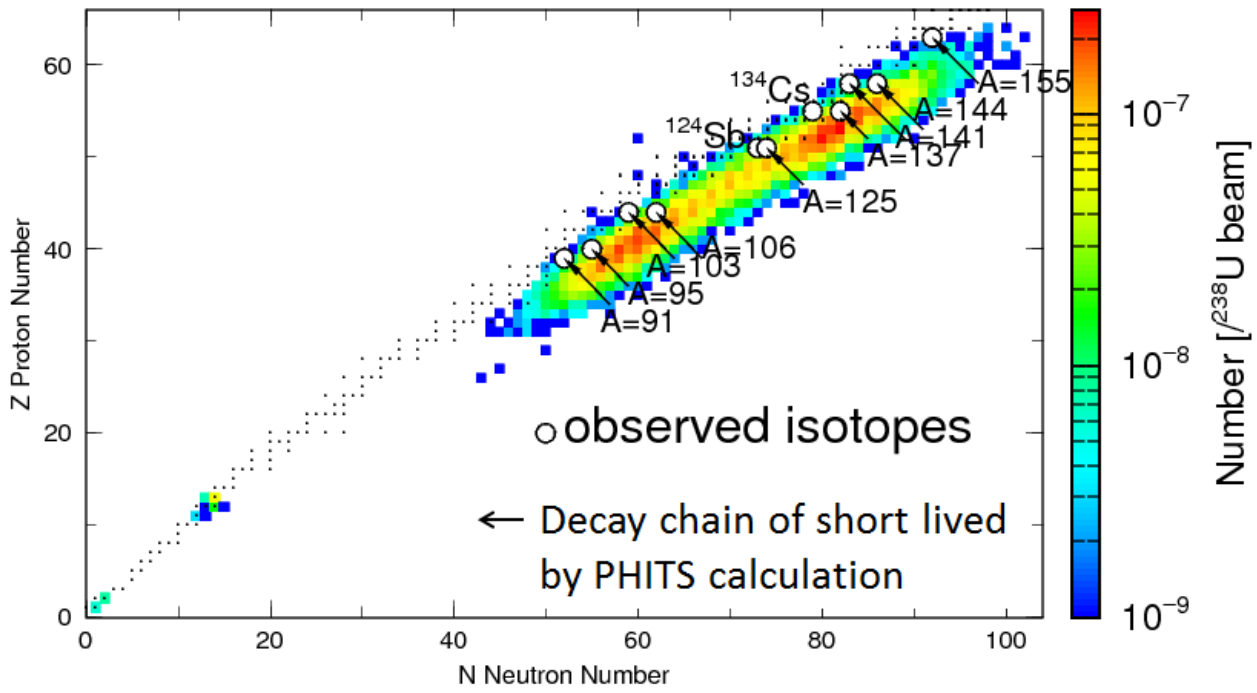

Figure 8. Nuclear chart of produced nuclei stopped at the Al-1a sample. The black dots indicate stable nuclei. The open circles show observed long-lived daughter nuclei, as listed in Table 1. The arrows indicate decay chains to the daughter nuclei evaluated by PHITS. Long-lived ^{124}Sb and ^{134}Cs do not have parent nuclei, because their $Z = +1$, $N = -1$ nuclei are stable. The ^{124}Sb and ^{134}Cs nuclei were therefore used to make a direct comparison between the results of the PHITS calculation to the measured values.

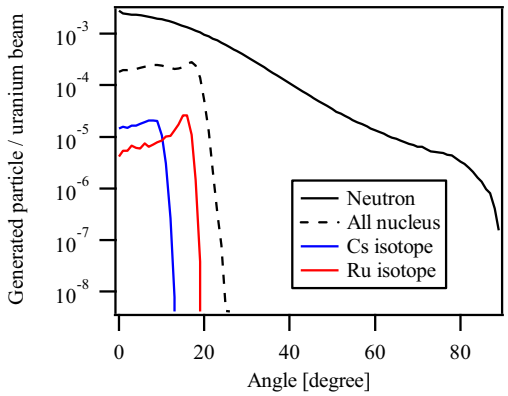

Figure 9. Angular distribution of produced neutron and fission product nuclei calculated by PHITS. 0.7 g/cm^2 helium target of 1-mm thickness was set for the calculation.

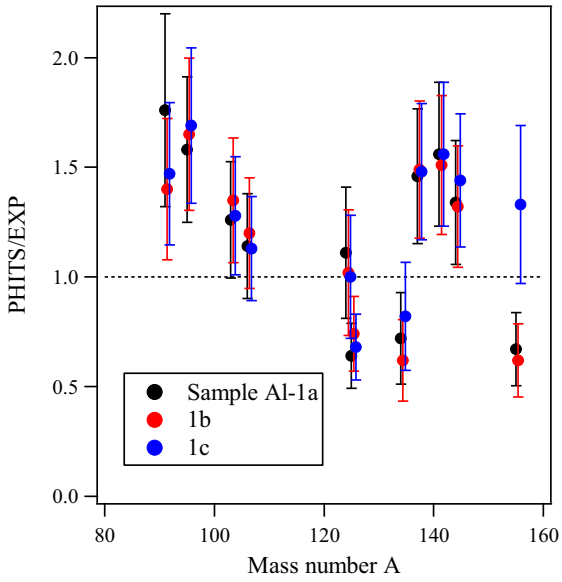

Figure 10. Ratios of calculated fission products to observed them.

4 Conclusion

Figure 9 shows the ratios of the numbers of nuclei calculated by PHITS calculations to the observed numbers of nuclei at the samples. The errors in the plots arose mainly from statistics of the γ-ray and PHITS calculations, and the 20% variation in accuracy of the beam intensity. The fission products stopped inside the aluminium sample first layers are shown. Evaluations of the neutron activation of the aluminium and bismuth samples are ongoing.

In this study, the results of the PHITS evaluation for fission products from a uranium beam at around 11 A MeV agreed within a factor of two with the measured values for all mass regions. Previously, K. Tanaka et al. measured sample activation by neutrons around a copper beam dump irradiated by a uranium beam at 345 A MeV at RIBF [7]. N. Nakao also measured neutron production through irradiation of a beryllium target at RIBF by a uranium beam at 345 A MeV by using bismuth samples placed from 60 to 90 degree of the target [8]. The results of their PHITS calculation for the activation ratio also agreed with the measured values. K. Kusaka et al. measured heat load by neutron and charged particles from the target on the first superconducting quadrupoles magnet at RIBF. The measured result of radiation heat load by a uranium beam at 345 A MeV also agreed with that of PHITS calculation [9]. D. Sato et al. and K. Niita et al. studied other beam nuclides for a beam of more than 100 A MeV [6, 10], and PHITS reproduced these measurements within a factor of two. For the case of low-energy reactions, Y. Iwamoto et al. measured the angular distribution of neutrons from a ^{9}Be target irradiated with a 10 MeV beam of protons and deuterons [11], and the neutron production in the forward angles calculated by PHTIS agreed with the experimental value. In the current uranium study, the calculated result for uranium fission agreed with the results of these previous studies for other nuclides and beam energies. Further evaluations of neutron activation for aluminium and bismuth samples are necessary.

Acknowledgement

The PHITS calculation was performed by using the RIKEN HOKUAI–GreatWave system, which permits rapid large-scale computations. The authors thank RIKEN for supporting the computing systems essential for the completion of this work. We also grateful to the accelerator operation staff and the experimental group of RIBF for helpful support in the parasitic experiment.

References

1. Y. Yano, Nucl. Instrum. Methods Phys. Res., Sect. B, **261** 1009 (2007); DOI: 10.1016/j.nimb.2007.04.174.
2. H. Imao, H. Okuno, H. Kuboki, et al., *Proceedings of IPAC2013,* 12–17th May 2013, Shanghai China, 3851–3853 (2013); http://accelconf.web.cern.ch/accelconf/IPAC2013/papers/thpwo038.pdf (Accessed 24th Oct. 2016).
3. T. Sato, K. Niita, N. Matsuda, et al., J. Nucl. Sci. Technol. (Abingdon, U. K.) **50**, 913 (2013); DOI: 10.1080/00223131.2013.814553
4. R. Koyama, N. Sakamoto, M. Fujimaki, et al., Nucl. Instrum. Methods Phys. Res., Sect. A, **729**, 788 (2013); DOI: 10.1016/j.nima.2013.08.056.
5. K. Shibata, O. Iwamoto, T. Nakagawa, N. Iwamoto, A. Ichihara, S.Kunieda, S. Chiba, K. Furutaka, N.Otsuka, T. Ohsawa, T. Murata, H. Matsunobu, A. Zukeran, S. Kamada, and J. Katakakura, J. Nucl. Sci. Technol. (Abingdon, U. K.) **48**, 1 (2011); DOI: 10.1080/18811248.2011.9711675
6. D. Sato , T. Kurosawa, T. Sato, A. Endo, M. Takada, H. Iwase, T. Nakamura, K. Niita, Nucl. Instrum.

Methods Phys. Res., Sect. A, **583** 507 (2007); DOI: 10.1016/j.nima.2007.09.23.
7. K. Tanaka, N. Inabe, K. Yoshida, T. Kubo, Prog. Nucl. Sci. Technol. **4**, 201 (2014); DOI: 10.15669/pnst.4.201.
8. N. Nakao, Y. Uwamino, K. Tanaka, *Proceedings of IPAC2014*, 15–20th June 2014, Dresden, Germany, 1811–1813 (2014); http://accelconf.web.cern.ch/AccelConf/IPAC2014/papers/tupri101.pdf?n=IPAC2014/papers/tupri101.pdf (Accessed 24th Oct 2016).
9. K. Kusaka M. Ohtake, K. Tanaka, K. Yoshida, and T. Kubo, IEEE Transactions and Applied Superconductivity, **25**, Issue3, 4100404 (2015); DOI: 10.1109/TASC.2014.2365957.
10. K. Niita, T. Sato, H. Iwase, H. Nose, H. Nakashima, L. Sihver, Radiat. Meas., **41** 1080 (2006); DOI: 10.1016/j.radmeas.2006.07.013.
11. Y. Iwamoto, Y. Sakamoto, N. Matsuda, et al. Nucl. Instrum. Methods Phys. Res., Sect. A, **598** 687 (2009); DOI: 10.1016/j.radmeas.2006.07.013.